Total β-electron spectra of ^{214}Pb and ^{214}Bi

Marlom Ramalho* and Jouni Suhonen†

*University of Jyväskylä, Department of Physics, P.O. Box 35, FI-40014 Jyväskylä, Finland
†University of Jyväskylä, Department of Physics, P.O. Box 35, FI-40014 Jyväskylä, Finland, and
International Centre for Advanced Training and Research in Physics (CIFRA), P.O. Box MG12, 077125
Bucharest-Magurele, Romania

Abstract. Beta electrons (electrons emitted in β decays) are a common background in rare-events experiments searching for beyond-the-standard-model physics in double beta decays, in dark-matter detection, etc. One particular culprit for the background events are the ^{220,222}Rn radioactive chains leading to β^- decays of ^{212,214}Pb and ^{212,214}Bi, common contaminants in the rare-events experiments. We have computed the total β-electron spectra of these decays using a state-of-the-art β-decay theory. The β decays involve numerous first-forbidden non-unique transitions depending strongly on the wave functions of the decay mother and daughter nuclei through the many involved nuclear matrix elements (NME). These NME have been computed by using the interacting shell model (ISM) with the *khpe* effective Hamiltonian. This Hamiltonian leads to a nice description of the energy spectra of the involved nuclei. We are able to reproduce the measured branching ratios of all the decay transitions by adopting the small relativistic NME (sNME) as a fit parameter. Here we report detailed results for the decays of ^{214}Pb and ^{214}Bi. We are confident that these calculations help the present and future rare-events experiments better identify their β-electron backgrounds stemming from the radon β-decay chains.

Keywords: beta decay, electron spectral shapes, total electron spectra
PACS: 21.60.Jz, 23.40.Bw, 23.40.Hc, 27.60.+j

INTRODUCTION

Nuclear β decay is a ubiquitous process of varying complexity. The simplest are the allowed β decays: Fermi and Gamow-Teller transitions which involve no orbital angular momentum of the emitted leptons [1]. In our cases of interest the leptons are the electron and electron antineutrino following a β^- decay. Decays involving higher partial waves of the emitted leptons are called forbidden, though they are not completely forbidden, but retarded by some three order of magnitude by every unit increase of forbiddenness, i.e. increase of one unit of orbital angular momentum of the leptons [2]. The Fermi and Gamow-Teller decays involve just one nuclear matrix element (NME) which depends on the transition operator and the wave functions of the mother and daughter nuclei of the decay. This leads to a universal shape of the energy distribution of the emitted electrons, depending only on the well-calculable lepton phase space. The same is true for the forbidden unique β transitions which also depend on just one NME. The β spectral shape of the forbidden non-unique β transitions depends on several NME and thus depends on the wave functions of the mother and daughter nuclei in a highly non-trivial way.

In addition to the many NME, the (partial) half-life of the forbidden non-unique β transitions depend in a non-trivial way on the values of the weak vector and axial-vector couplings, $g_{\rm V}$ and $g_{\rm A}$, respectively [2]. The CVC (conserved vector current) hypothesis confines the value of the vector coupling to $g_{\rm V} = 1.0$ whereas the PCAC (partially conserved axial-vector current) hypothesis leaves the so-called effective value of $g_{\rm A}$ in finite nuclei uncertain [3], the bare-nucleon value being around $g_{\rm A} = 1.27$, obtained from the decay of an isolated neutron to a proton, electron and electron antineutrino. The quenching of the effective value of $g_{\rm A}$ has been studied a lot (see the recent reviews [3, 4, 5]), in particular its effects on the neutrinoless double beta decay [6, 7].

In addition to quenching, an enhancement of $g_{\rm A}$, based on two-body meson-exchange currents has been recorded for first-forbidden non-unique (ff-nu) β transitions with no angular-momentum change [5, 8]. All these facets of the axial coupling carry over to the theoretical analyses of the β-spectral shapes and their comparison with the available experimental data, like in the recent spectral-shape analyses of [9, 10, 11, 12].

A particular role in the theoretical spectral-shape and half-life analyses is played by the so-called small relativistic NME, the sNME. Despite its smallness, sNME can influence the β spectral shapes and half-lives quite strongly [10, 12, 13]. The sNME gathers contributions outside the valence major shell where the proton and neutron Fermi surfaces lie. This makes its calculation particularly hard for a nuclear model like the interacting shell model (ISM)

which typically uses as valence space just those major shells which contain the nucleon Fermi surfaces.

Combined experimental and theoretical analyses of β-spectral shapes of individual β transitions have been done recently [9, 10, 11, 12], but analyses of total β spectra, constructed from all the individual β transitions falling within a β-decay Q window of several MeV (excitation-energy range in the β-decay daughter nucleus allowed by the available decay energy Q) are few: The analysis of the ^{92}Rb β^- decay in connection with the reactor antineutrino anomalies [14] and the analyses of [13] in connection with the β-decay contaminants in the ^{220,222}Rn radioactive chains. In the present paper we detail and complement some of the β spectral analyses for the decays of ^{214}Pb and ^{214}Bi, published originally in [13].

OUTLINE OF THE THEORETICAL ASPECTS

The half-life of a β transition can be obtained from $t_{1/2} = \kappa/\tilde{C}$, where κ is a constant [15, 16] and $\tilde{C}$ is the integrated shape function, discussed in detail in [17, 18]. The main focus in the present paper are the ff-nu β transitions associated with parity change and angular-momentum changes $\Delta J = 0$ (corresponding to a pseudoscalar operator) and $\Delta J = 1$ (a pseudovector operator involved). In addition, the $\Delta J = 2$ (a pseudotensor operator involved) are present, but the corresponding β spectral shape is universal as explained in the introduction. The $\Delta J = 2$ transitions are purely axial-vector, but the $\Delta J = 0, 1$ transitions are both vector and axial-vector.

In the present ISM calculations, we choose the value $g_{\rm A} = 0.85$ used earlier in an ISM-based β-decay analysis of ^{214}Pb by Haselschwardt *et al.* [19]. The $\Delta J = 0$ transitions are characterized by an enhancement factor $\varepsilon_{\rm MEC}$ [8] leading to an enhanced axial coupling $g_{\rm A}(\gamma_5) = \varepsilon_{\rm MEC} g_{\rm A}$. Here we adopt the value $g_{\rm A}(\gamma_5) = 2.437 \pm 0.014$, as obtained in the analysis of [13].

The ISM calculations were performed using the software KSHELL [20] with the ISM Hamiltonian *khpe* [21] in a valence space consisting of the proton $1h_{9/2}$-$2f_{7/2}$-$2f_{5/2}$- $3p_{3/2}$-$3p_{1/2}$ orbitals and the neutron $1i_{11/2}$-$2g_{9/2}$-$2g_{7/2}$-$3d_{5/2}$-$3d_{3/2}$-$4s_{1/2}$-$1j_{15/2}$ orbitals. No truncations of the many-nucleon configuration space were made. Experimental Q values were adopted, along with measured excitation energies of the β-decay daughter nuclei.

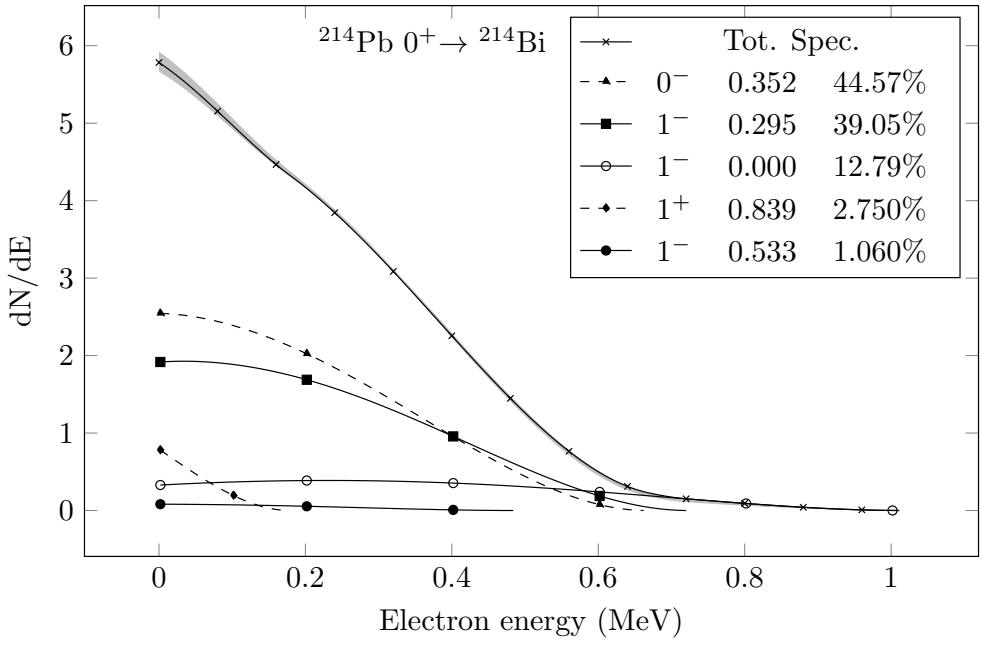

FIGURE 1. Computed total β spectrum (within the gray-hatched region) of the decay ^{214}Pb$(0^+) \rightarrow$ ^{214}Bi and its major individual contributions, obtained with the sNMEs closest to their CVC values. The total spectrum with all possible combinations of sNMEs builds the gray-hatched stripe.

RESULTS AND DISCUSSION

Here we present and discuss the results for the ff-nu β-decay transitions $^{214}\mathrm{Pb}(0^+) \rightarrow {}^{214}\mathrm{Bi}(0^-, 1^-)$ and $^{214}\mathrm{Bi}(1^-) \rightarrow {}^{214}\mathrm{Po}(0^+, 1^+, 2^+)$. For the ^{214}Pb decay the experimental branchings to the lowest 0^- and 1^- states of ^{214}Bi are the largest (44.5% and 39.0%, respectively), whereas for the ^{214}Bi decay the experimental branching to the 0^+ ground state of ^{214}Po is the largest, with 19.2%. However, there are several transitions that have branchings within the range from a few percent to 17.5%.

In the calculations the starting point is the determination of the proper value of the sNME. The CVC value of it can be obtained by relating [2] its value to the value of the so-called large vector NME, l-NME, well calculable using the ISM since by far most of its contributions stem from major shells containing the proton and neutron Fermi surfaces. In the present study we use the CVC value of the sNME as a reference and, instead, determine the value of the sNME by reproducing the experimental branching (or, equivalently, the partial half-life) of each of the ff-nu β transitions contained in the β-decay Q window. In fact, there are two values of the sNME which reproduce the measured branching [10, 12, 13]. In some cases the dependence of the electron spectral shape on the value of the sNME is quite strong, like in the case of the $^{212}\mathrm{Bi}(1^-) \rightarrow {}^{212}\mathrm{Po}(2_2^+)$ transition to the second excited 2^+ state [13] and through that it can also affect strongly the total β spectral shape.

In Figs. 1 and 2 we present our results for the total β spectra of ^{214}Pb and ^{214}Bi, with their major decompositions into individual transitions. The spectral curves within the shaded regions correspond to the values of sNME closest to their CVC values. The shaded region includes all the possible combinations of sNMEs for the transitions building up the total β spectrum, thus representing an error estimate for the total spectrum. For the decays of ^{214}Pb and ^{214}Bi this error band is quite narrow, as shown in Figs. 1 and 2. As can be seen in Fig. 1, decays to the lowest 0^- and 1^- states of ^{214}Bi dominate the total β spectrum of ^{214}Pb, whereas for ^{214}Bi (Fig. 2) several transitions contribute rather equally, the decay to the 0^+ ground state of ^{214}Po dominating at electron energies above some 1 MeV and the transition to the first 2^+ state, at 1.729 MeV of excitation, dominating below that. At very low electron energies the contributions of a plethora of high-lying excited states (more than 30 states contributing with a total branching of some 10%) dominate.

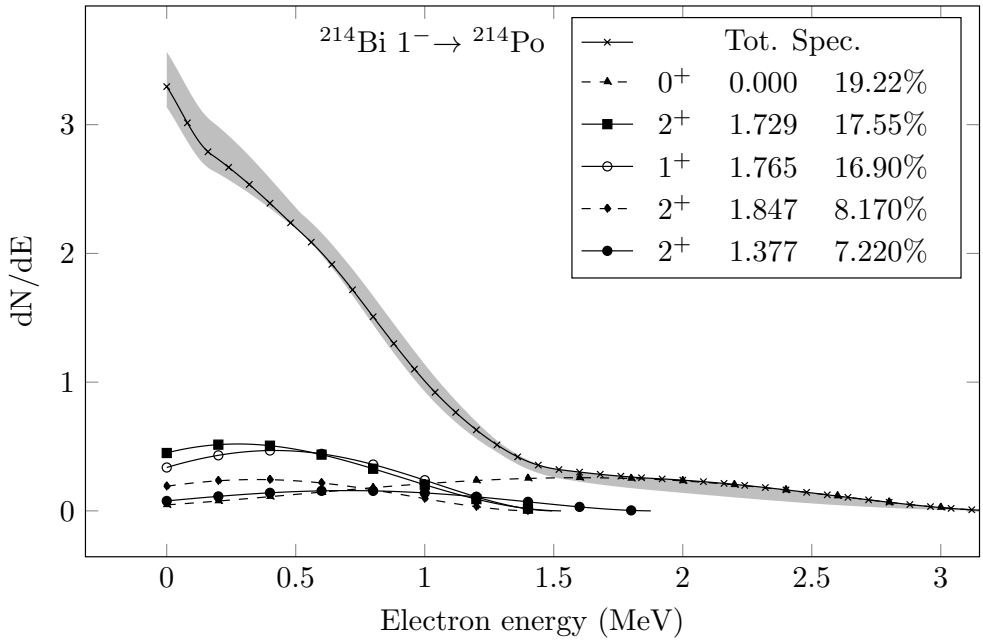

FIGURE 2. Computed total β spectrum of the decay $^{214}\mathrm{Bi}(0^+) \rightarrow {}^{214}$Po and the five highest contributions to the spectrum. For more details, see the caption of Fig. 1.

SUMMARY AND CONCLUSIONS

Calculation of β-electron spectra related to various radioactive chains for the many running and future rare-events experiments is of high priority. Notorious cases consist of the ^{220,222}Rn radioactive chains containing β^- decaying lead and bismuth nuclei. In the present work we concentrate on the ^{222}Rn chain and analyses of the β-electron spectra of ^{214}Pb and ^{214}Bi related to β^- transitions to excited states in the respective daughter nuclei ^{214}Bi and ^{214}Po. For the ^{214}Pb decay only a few transitions dominate the total spectrum whereas for the ^{214}Bi decay several transitions take part in forming the total β spectrum. It is our hope that these results will help the present and future rare-events experiments better identify these β-decay contaminants in their searches for beyond-the-standard-model physics.

REFERENCES

1. J. Suhonen, *From Nucleons to Nucleus: Concepts of Microscopic Nuclear Theory* (Springer-Verlag Berlin Heidelberg, Springer, Gaithersburg MD, 20899, 2007).
2. H. Behrens and W. Bühring, *Electron Radial Wave Functions and Nuclear Beta-decay (International Series of Monographs on Physics)* (Clarendon Press, Oxford, 1982).
3. J. Suhonen, *Front. Phys.* **5**, 55 (2017).
4. J. Suhonen and J. Kostensalo, *Front. Phys.* **7**, 29 (2019).
5. H. Ejiri, J. Suhonen, and K. Zuber, *Phys. Rep.* **797**, 1 (2019).
6. J. Engel and J. Menendez, *Rep. Prog. Phys.* **60**, 046301 (2017).
7. M. Agostini, G. Benato, J. A. Detwiler, J. Menéndez, and F. Vissani, *Rev. Mod. Phys.* **95**, 025002 (2023).
8. J. Kostensalo and J. Suhonen, *Phys. Lett. B* **781**, 480 (2018).
9. L. Bodenstein-Dresler *et al.* (The COBRA Collaboration), *Phys. Lett. B* **800**, 135092 (2020).
10. J. Kostensalo, J. Suhonen, J. Volkmer, S. Zatschler, and K. Zuber, *Phys. Lett. B* **822**, 136652 (2021).
11. A. F. Leder *et al.*, *Phys. Rev. Lett.* **129**, 232502 (2022).
12. J. Kostensalo, E. Lisi, A. Marrone, and J. Suhonen, *Phys. Rev. C* **107**, 055502 (2023).
13. M. Ramalho and J. Suhonen, Submitted to *Phys. Rev. C* (2023).
14. M. Ramalho, J. Suhonen, J. Kostensalo, G. A. Alcalá, A. Algora, M. Fallot, A. Porta, and A.-A. Zakari-Issoufou, *Phys. Rev. C* **106**, 024315 (2022).
15. A. Kumar, P. C. Srivastava, J. Kostensalo, and J. Suhonen, *Phys. Rev. C* **101**, 064304 (2020).
16. A. Kumar, P. C. Srivastava, and J. Suhonen, *Eur. Phys. J. A* **57**, 225 (2021).
17. M. Haaranen, P. C. Srivastava, and J. Suhonen, *Phys. Rev. C* **93**, 034308 (2016).
18. M. Haaranen, J. Kotila, and J. Suhonen, *Phys. Rev. C* **95**, 024327 (2017).
19. S. J. Haselschwardt, J. Kostensalo, X. Mougeot, and J. Suhonen, *Phys. Rev. C* **102**, 065501 (2020).
20. N. Shimizu, T. Mizusaki, Y. Utsuno, and Y. Tsunoda, *Comp. Phys. Comm.* **244**, 372 (2019).
21. E. K. Warburton, *Phys. Rev. C* **44**, 233 (1991).